East European Journal of Physics. 2. 352–360 (2026)
DOI: 10.26565/2312-4334-2026-2-37 ISSN 2312-4334

FINITE ELEMENT MODELING OF SCANNING SPEED EFFECTS IN FEMTOSECOND LASER-INDUCED GRAPHENE FABRICATION

J.O. Sadullayev[1], **M.M. Akhmedov**[1*], **M.E. Vapayev**[1], **A.E. Rajabov**[1], **I.Y. Davletov**[1], **G.S. Boltaev**[2]
[1]*Department of Electrical Engineering and Power Engineering, Urgench State University named after Abu Raykhan Beruni, Urgench, 220100, Uzbekistan*
[2]*Department of Physics, American University of Sharjah, Sharjah 26666, United Arab Emirates*
[*]*Corresponding Author e-mail: munisbek95@urdu.uz*
Received February 22, 2026; revised April 4, 2026; accepted April 8, 2026

Laser-induced graphene (LIG) enables mask free direct writing of conductive carbon structures on polyimide substrates for flexible electronic and sensing applications. In femtosecond laser-induced graphene (FLIG), the scanning speed strongly affects the local temperature field, and thus the extent and quality of graphitization, but this dependence is still not fully quantified. In this study, a time dependent finite element model is implemented in COMSOL Multiphysics to resolve the temperature distribution generated by a femtosecond laser beam on a polyimide surface as a function of scanning speed. The laser is described as a moving Gaussian surface heat source, and the transient heat conduction equation is solved to capture ultrafast heating and cooling during a pulse train. Simulations for scan speeds between 0.05 and 0.20 m/s show that decreasing the speed increases the peak temperature and enlarges the heat affected zone, whereas higher speeds reduce both quantities. By comparison of the predicted peak temperatures with the graphitization thresholds in the literature for polyimide derived graphene, an intermediate scan speed window is identified in which the thermal budget is sufficient for graphene formation while avoiding excessive overheating and damage. This modeling framework provides a practical tool for pre selecting femtosecond laser parameters and for accelerating the optimization of FLIG processes for flexible graphene based devices.

Keywords: *Laser-induced graphene; Polyimide; Scanning speed; Ultrafast heat transfer; Moving Gaussian heat source; Finite element modeling; Temperature distribution; Graphitization window*

PACS: 42.70.Hj, 42.62.Fi

1. INTRODUCTION

Laser-induced graphene (LIG) has emerged as a versatile and scalable technique for the direct writing of conductive graphene-like networks on polymer substrates due to its simplicity, mask-free patterning capability, and compatibility with large-area processing. Typically, LIG is synthesized by scanning a focused laser beam across a carbon-rich precursor such as polyimide, where localized photothermal conversion induces carbonization and graphitization, resulting in a porous turbostratic graphene structure with tunable morphology and electrical conductivity [1–5]. These unique structural and electrical properties, combined with the ability to fabricate arbitrary planar geometries, have enabled numerous applications in flexible and wearable electronics, including strain sensors, pressure sensors, and biointerfaces [6–9]. Furthermore, the high specific surface area and excellent electrical conductivity of LIG make it particularly attractive for energy harvesting and storage applications, such as microsupercapacitors and electrochemical electrodes [10–12].

More recently, femtosecond laser processing has been introduced as an advanced approach to improve the spatial confinement of laser energy deposition and minimize collateral thermal damage. Ultrafast laser pulses can induce nonlinear absorption and highly localized energy transfer, leading to rapid heating and graphitization while significantly reducing heat diffusion into surrounding material regions [13–16]. As a result, femtosecond laser-induced graphene (FLIG) often exhibits improved structural uniformity, higher electrical conductivity, and enhanced material quality compared to graphene produced using continuous wave or long-pulse lasers [13]. However, FLIG formation is highly sensitive to laser processing parameters, including laser power, repetition rate, scanning speed, and hatch spacing. These parameters strongly influence the thermal history of the material and determine whether graphitization, partial carbonization, or material ablation occurs [10, 16].

In many previous studies, optimization of laser processing parameters—particularly scanning speed—has been performed using empirical approaches or design-of-experiments methodologies to balance electrical performance, structural integrity, and fabrication throughput [17–26]. Although these experimental approaches are effective for identifying suitable processing windows, they often require extensive experimental effort and do not provide direct insight into the underlying thermal mechanisms governing graphene formation. In ultrafast laser processing regimes, direct experimental measurement of transient temperature fields at the laser–material interface is extremely challenging due to the short timescales involved. Therefore, numerical modeling has become an essential tool for investigating ultrafast laser–material interactions. Time-dependent heat transfer simulations based on the finite element method (FEM) have been successfully

Cite as: J.O. Sadullayev, M.M. Akhmedov, M.E. Vapayev, A.E. Rajabov, I.Y. Davletov, G.S.Boltaev, East Eur. J. Phys. 2, 352 (2026), https://doi.org/10.26565/2312-4334-2026-2-37

applied to laser processing problems and can be extended to femtosecond laser irradiation by incorporating appropriate heat source formulations and ultrafast heat transfer models [27–29].

COMSOL Multiphysics provides a powerful and flexible framework for implementing such models, including moving Gaussian heat sources and advanced heat transfer formulations suitable for ultrafast laser–material interactions [27, 29]. By representing the femtosecond laser beam as a moving Gaussian surface heat flux on a polymer substrate, it is possible to simulate the spatiotemporal evolution of temperature distributions under different scanning speeds while maintaining constant laser parameters [28, 29]. From these simulations, key physical quantities such as peak temperature, thermal gradients, heat-affected zone dimensions, and cooling dynamics can be extracted and correlated with the experimental conditions required for graphene formation. This combined numerical and experimental approach provides a rational foundation for optimizing the processing parameters and improving the efficiency and quality of FLIG fabrication [13, 17, 26, 40, 43].

In this work, a numerical investigation of the evolution of temperature during femtosecond laser-induced graphene formation on a polymer substrate is presented, with particular emphasis on the effected of laser scanning speed. A time-dependent finite element model is developed in COMSOL Multiphysics using a moving Gaussian heat source to represent laser irradiation [28, 29]. The model is used to evaluate the influence of scanning speed on peak temperature, spatial temperature distribution, and thermal relaxation behavior. The results provide fundamental insight into the thermal mechanisms governing femtosecond laser-induced graphene formation and offer practical guidance for selecting optimal laser processing parameters for controlled and efficient FLIG fabrication.

In addition, the obtained results are consistent with analytical and mathematical approaches reported in recent studies on semiconductor structures, where the influence of temperature and material parameters on electronic and thermal characteristics has been systematically investigated [30–39], further confirming the reliability of the developed finite element model for describing temperature-dependent processes.

In this context, the present work makes three specific contributions.First, it establishes a systematic finite element model to quantify how femtosecond laser scanning speed controls the full spatiotemporal temperature field during laser-induced graphene formation on polymer substrates. Second, the model is used to identify a scan speed window in which the peak temperature and heat affected zone dimensions are compatible with graphene formation, thus providing a thermally grounded definition of an "optimal" processing regime. Third, the simulated temperature metrics are formulated in a way that can be directly correlated with experimentally accessible indicators such as Raman signatures, sheet resistance, and morphology, offering a practical route to integrate numerical predictions with future femtosecond FLIG optimization studies.

2. METHODOLOGY

2.1. Geometrical Model and Material Properties

The numerical simulations were performed in COMSOL Multiphysics using a two-dimensional representation of a polyimide (PI) substrate irradiated by a scanning femtosecond laser beam. The substrate was modeled as a rectangular domain with a thickness of $H_1 = 1.29 \times 10^{-4}$ m and a width of $W_1 = 2.0 \times 10^{-3}$ m. These dimensions represent a typical PI film geometry, while ensuring that the lateral boundaries remain sufficiently far from the heated region to minimize edge effects on the computed temperature field.

The initial temperature of the entire domain was set equal to the ambient temperature, $T_a = 293.15$ K.

Temperature-dependent thermophysical properties of polyimide—namely density (ρ), specific heat capacity (C_p), and thermal conductivity (k)—were obtained from literature and the COMSOL material library over the temperature range from room temperature up to the onset of carbonization.

Convective heat transfer to the surrounding air was modeled on the exposed surfaces using a heat transfer coefficient of $h_1 = 17\,\mathrm{W\,m^{-2}\,K^{-1}}$. Radiative heat losses were also taken into account using a surface emissivity of $\varepsilon = 0.7$. These parameters are consistent with previous numerical studies on laser heating of polymeric substrates and provide a realistic approximation of typical laboratory conditions.

2.2. Governing Equation and Assumptions

Heat transfer in the PI substrate was described by the transient heat-conduction equation in the lattice (continuum) approximation,

$$\rho C_p \frac{\partial T}{\partial t} = \nabla \cdot (k \nabla T) + Q(x, y, t), \tag{1}$$

where T is the temperature and $Q(x, y, t)$ denotes the volumetric heat source associated with laser absorption.

Given the spatial and temporal scales considered (spot radius on the order of 10^{-4} m and pulse duration $P_w = 250$ fs), classical Fourier conduction was adopted as a first-order approximation; non-Fourier or two-temperature descriptions may be incorporated in future work to capture electron–phonon nonequilibrium more rigorously. Phase change, ablation, and temperature-dependent variations in optical properties were neglected so that the model isolates the role of scanning-speed-controlled thermal fields within the regime relevant to the onset of graphitization.

2.3. Laser Heat Source and Scanning Motion

The femtosecond laser was modeled as a train of Gaussian pulses incident on the upper surface of the substrate. The pulse repetition rate was set to $f = 10$ kHz, leading to an average power P_{avg} delivered to the surface. The beam was characterized by a diameter $D = 100\ \mu$m ($1/e^2$ intensity width), corresponding to a beam radius $w_0 = D/2 = 50\ \mu$m. The laser operated at a central wavelength of $\lambda = 1060$ nm. An effective absorptivity $A_1 = 0.8$ was assumed for the PI surface at this wavelength, such that the absorbed power entering the thermal model is $P_{\text{abs}} = A_1 P_{\text{avg}}$. The temporal width of each pulse was $P_{\text{w}} = 250$ fs, implemented as a short top-hat function within each $1/f$ period to approximate femtosecond energy deposition followed by longer-time heat diffusion.

The spatial distribution of the absorbed heat flux at the surface was described by a moving Gaussian profile,

$$q(x, y, t) = \frac{2P_{\text{abs}}}{\pi w_0^2} \exp\left(-\frac{2\big(x - x_c(t)\big)^2 + 2\big(y - y_c\big)^2}{w_0^2}\right) g(t), \tag{2}$$

where $(x_c(t), y_c)$ denotes the instantaneous beam center and $g(t)$ specifies the temporal envelope of the pulse train. The beam center followed a linear trajectory along the x-direction,

$$x_c(t) = x_0 + vt, \tag{3}$$

with $x_0 = D$ used as the reference entrance position and v denoting the scanning speed. In this work, v was varied between 0.05 and 0.20 m/s, while all other laser parameters were kept constant. This moving-source description was implemented in COMSOL Multiphysics via analytic functions defining the Gaussian heat flux and a time-dependent boundary condition applied at the top surface.

2.4. Boundary and Initial Conditions

At $t = 0$, the temperature throughout the substrate was set to the ambient value $T_a = 293.15$ K. The top surface received the laser heat flux described in Section 2, in addition to convective and radiative heat losses. The lateral boundaries were treated as adiabatic, reflecting the assumption that the computational domain is sufficiently wide to minimize lateral heat leakage over the time scales of interest. The bottom surface was coupled to the environment through convection and radiation, approximating thermal contact with a support stage exposed to air.

3. RESULTS AND ANALYSIS

Time-dependent COMSOL Multiphysics simulations were employed to quantify how the femtosecond laser scanning speed governs the spatial and temporal evolution of the temperature field during laser-induced graphene formation. Figures 1-4 present the surface temperature distributions along the laser track for scan speeds of 0.05, 0.10, 0.15, and 0.20 m/s, respectively. A clear monotonic trend is observed: decreasing the scanning speed substantially increases the peak temperature and broadens the thermally affected zone, whereas higher speeds lead to more confined and cooler heating profiles.

Figure 1. Simulated temperature distribution at a scanning speed of 0.20 m/s (peak surface temperature $T_{\text{max}} \approx$ 2400 K). At 0.20 m/s, the train of femtosecond pulses produces a sequence of sharp temperature spikes that cumulatively drive the surface temperature to a quasi-steady peak around 2400 K. This peak remains slightly below the $\approx$ 2500 K level typically associated with the formation of well-ordered graphene domains, so the local thermal budget is sufficient for graphitization but not ideal for extensive defect healing. Consequently, the resulting graphene layer along the scan track is expected to be at least partially defective, with a higher density of structural imperfections compared with layers formed under conditions where the peak temperature significantly exceeds 2500 K.

Figure 2. Simulated temperature evolution at a scanning speed of 0.15 m/s (peak surface temperature $T_{\text{max}} \approx 2480$ K). At 0.15 m/s, the sequence of femtosecond pulses leads to a progressive build-up of temperature, and the surface repeatedly experiences sharp spikes that rise to a maximum of about 2480 K. This peak value lies very close to the lower bound of the $\approx$ 2500–3500 K window associated with the formation of well-developed graphene networks in polyimide-derived LIG [41]. Consequently, the local thermal conditions at this speed are expected to support more extensive graphitization and partial defect healing compared with 0.20 m/s, although the graphene layer may still contain a noticeable density of structural imperfections relative to regimes where T_{max} comfortably exceeds 2500 K.

Figure 3. Simulated temperature evolution at a scanning speed of 0.10 m/s (peak surface temperature $T_{\text{max}} \approx 2500$ K). At 0.10 m/s, the femtosecond pulse train generates a sequence of sharp temperature spikes with noticeable cumulative heating, and the surface temperature gradually approaches a maximum of about 2500 K without exceeding this level for any of the pulses. Since 2500 K is close to the lower boundary of the graphitization window for polyimide-derived graphene, the thermal conditions at this speed are sufficient to support graphene formation along the scan track but only marginally adequate for pronounced defect healing. Consequently, the resulting graphene layer is expected to be relatively continuous yet still contain a considerable density of structural defects compared with regimes where T_{max} clearly exceeds the optimal graphitization range.

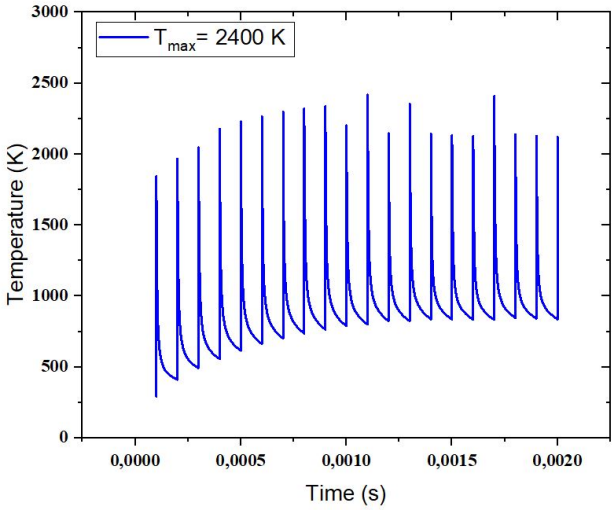

Figure 1. Temporal temperature evolution under pulsed laser irradiation at a scanning speed of 0.2 m/s (T_{max} = 2400 K)

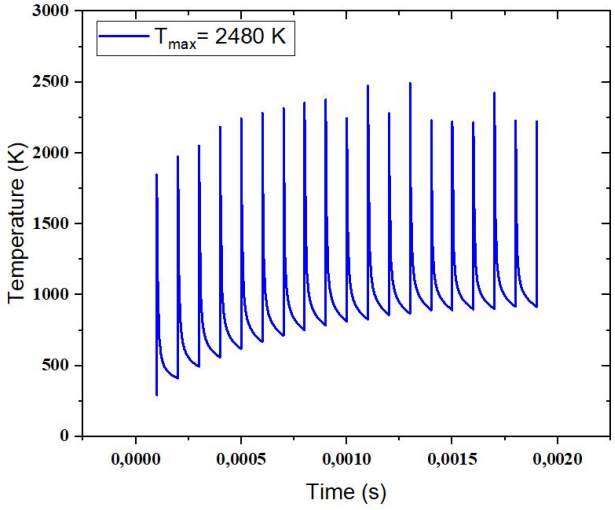

Figure 2. Temporal temperature evolution under pulsed laser irradiation at a scanning speed of 0.15 m/s (T_{max} = 2480 K)

Figure 4. Simulated temperature evolution at a scanning speed of 0.05 m/s (peak surface temperature $T_{max} \approx$ 2600 K). At this lowest scanning speed, the laser–material interaction time is longest, so the cumulative effect of successive femtosecond pulses leads to a strong build-up of temperature and a maximum surface value of about 2600 K. This peak lies clearly inside the 2500–3500 K graphitization window reported for polyimide-derived graphene, indicating that the thermal conditions are highly favorable for the formation of a well-developed graphene network and for partial annealing of pre-existing defects. However, the pronounced heat accumulation also implies a wider heat-affected zone and a higher risk of local overheating or ablation in comparison with higher scanning speeds, which may compromise fine feature control even though the graphene layer quality is expected to be relatively high along the scan track.

Figure 5 presents the dependence of the maximum surface temperature T_{max} on the laser scanning speed in the range from 0.05 to 0.20 m/s. The curve shows a clear monotonic decrease: as the scanning speed is increased, the peak temperature achieved at the surface systematically drops from about 2600 K at 0.05 m/s to roughly 2400 K at 0.20 m/s. This trend is consistent with the reduced interaction time and lower effective energy input per unit length at higher scan speeds, which restrict heat accumulation in the polyimide substrate. At the lowest speed considered (0.05 m/s), T_{max} lies well inside the graphitization window 2500–3500 K, indicating favorable conditions for the formation of a well-developed

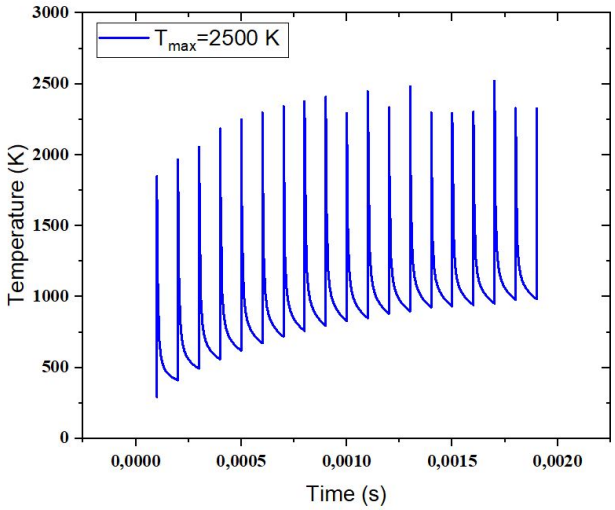

Figure 3. Temporal temperature evolution under pulsed laser irradiation at a scanning speed of 0.1 m/s ($T_{\max}$ = 2480 K)

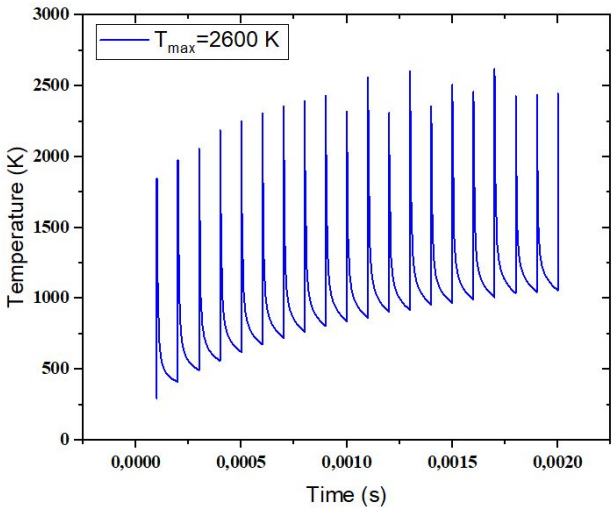

Figure 4. Temporal temperature evolution under pulsed laser irradiation at a scanning speed of 0.05 m/s ($T_{\max}$ = 2600 K)

graphene layer, while at 0.20 m/s the peak temperature falls closer to the lower boundary of this window and is expected to produce a thinner or more defective graphene film [41, 42]. The error bars in Figure 5 reflect the variation in peak temperature extracted from different probe locations along the scan track and highlight that, despite this variability, the overall decreasing trend with increasing scanning speed remains robust.

This trend aligns with the experimental findings of Murray et al. [16], where lower scanning speeds (e.g., 70–200 mm/s) produced high-quality LIG with low sheet resistance (~16 Ω/sq) and sharp Raman 2D peaks, indicating better graphitization. Our FEM model complements this by quantifying the underlying thermal mechanism: peak temperatures systematically decrease from 2600 K at 0.05 m/s to 2400 K at 0.20 m/s, defining a graphitization window of 2500–3500 K consistent with MD simulations in recent studies [41, 42].

The simulation results reveal a clear and systematic dependence of the transient thermal field on scanning speed, confirming that this parameter is a primary handle for controlling femtosecond laser-induced graphene formation on polyimide. At low scanning speeds, cumulative heating drives the peak surface temperature deep into the graphitization window and generates a wide heat-affected zone, which supports extensive carbonization but increases the risk of structural damage and local ablation. Intermediate speeds yield more moderate peak temperatures and tighter thermal footprints

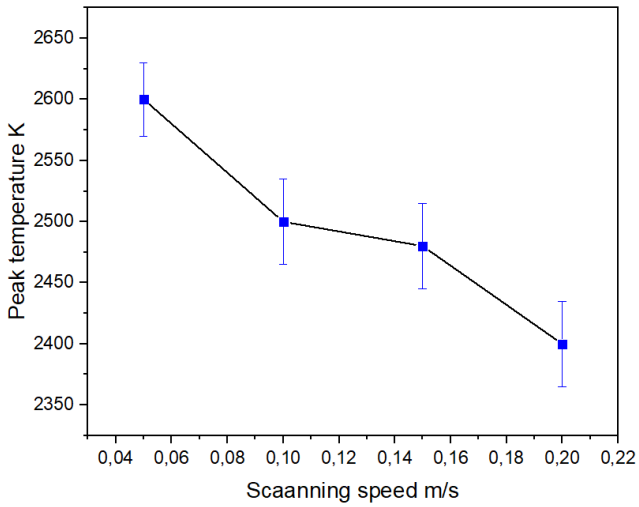

Figure 5. Peak surface temperature as a function of scanning speed (0.05–0.20 m/s).

while preserving a continuous high-temperature region along the scan path, making them particularly attractive as an operational window where graphene can form reliably with reduced thermal loading of the surrounding material. At the highest speeds considered, the thermal budget becomes marginal for robust graphitization, so although throughput is improved, the resulting graphene is expected to be thinner and more defective or even discontinuous along the track. Altogether, these observations delineate a finite scan-speed range in which the peak temperature and spatial extent of the heated zone jointly favor continuous, higher-quality graphene while limiting unnecessary overheating, and they provide a predictive basis for linking thermal metrics to future experimental measurements such as Raman spectra, sheet resistance, and morphology.

4. CONCLUSIONS

This study has established a time-dependent finite-element framework in COMSOL Multiphysics to quantify how femtosecond laser scanning speed governs the spatiotemporal temperature field during laser-induced graphene formation on polyimide. By modeling the laser as a moving Gaussian surface heat source and systematically varying the scanning speed in the range 0.05–0.20 m/s, the simulations revealed a monotonic decrease of the peak surface temperature from ≈ 2600 K at 0.05 m/s to ≈ 2400 K at 0.20 m/s, accompanied by a gradual contraction of the heat-affected zone. Comparison of these peak temperatures with reported graphitization windows for polyimide-derived graphene indicates that low and intermediate scan speeds fall within or close to the 2500–3500 K range associated with well-developed graphene networks, whereas higher speeds approach the lower bound of this window and are likely to produce thinner or more defective graphene layers.

The results therefore delineate a finite scan-speed window in which the thermal budget is sufficient to drive robust graphitization while limiting excessive overheating and damage. In practical terms, very low scanning speeds provide favorable conditions for high-quality graphene formation but at the cost of a wide heat-affected zone and an increased risk of ablation, whereas excessively high speeds enhance throughput but undermine graphene continuity and structural quality. Intermediate speeds, where peak temperatures lie safely within the graphitization window and the thermal footprint remains compact, emerge as promising candidates for defining an optimal processing regime for femtosecond laser-induced graphene.

From an application standpoint, the insights gained here are directly relevant to the design of FLIG-based flexible sensors, microsupercapacitor electrodes, and other planar graphene devices, where a balance between electrical performance, pattern resolution, and substrate integrity is critical. The presented modeling strategy can be used as a predictive tool to pre-screen scanning speeds and laser settings before fabrication, thereby reducing experimental iteration and accelerating process development. Future work should combine the thermal simulations with experimental characterization—such as Raman spectroscopy, sheet-resistance mapping, and microscopy—to quantitatively link the predicted temperature metrics to defect density and device performance, and to refine the graphitization thresholds for different polyimide grades and laser systems.

Acknowledgments

We acknowledge the F-FA-2021-510 Grant from the Ministry of Innovative Development of Uzbekistan.

ORCID

J.O. Sadullayev, https://orcid.org/0000-0002-5577-2644; **M.M. Akhmedov**, https://orcid.org/0000-0003-1208-1736;
M.E. Vapayev, https://orcid.org/0009-0007-5194-131X; **A.E. Rajabov**, https://orcid.org/0000-0003-1687-2113;
I.Y. Davletov, https://orcid.org/0009-0006-5971-7649; **G.S. Boltaev**, https://orcid.org/0000-0003-0354-1251

REFERENCES

[1] S. P. Lee, H. Kim, and J. Park, "A review on laser-induced graphene in flexible energy storage and conversion devices," Chem. Eng. J. **499**, 156110 (2024). https://doi.org/10.1016/j.cej.2024.156110.

[2] J. Yang, J. Yu, K. Zhang, F. Qiao, and G. Yu, "Laser-Induced Graphene Toward Flexible Energy Harvesting and Storage Electronics," Advanced Materials Technologies, **9**(22), 2301602 (2024). https://doi.org/10.1002/admt.202301602

[3] M. R. Bedilov, Kh. B. Beisembaeva, and I. Yu. Davletov, "Formation of the spectra of multiply charged ions from the plasma of Nd-doped glass irradiated with a neodymium laser," Technical Physics, **47**(8), 1019–1023 (2002). https://doi.org/10.1134/1.1501684

[4] Bedilov, M. R., Davletov, I. Y., Sabitov, M. S., Berdierov, G. R., Tsoi, T. G., "Multiply charged ion spectra of a laser plasma produced on both sides of the target," Quantum Electronics, **31**(5), 453 (2001). https://doi.org/10.1070/QE2001v031n05ABEH001977

[5] M. R. Bedilov, R. T. Khaidarov, B. K. Yakubov, and U. S. Kunishev, "Charge and energy spectra of multiply charged ions of a two-element laser plasma formed from targets of different densities," Quantum Electronics, **26**(9), 814 (1996). https://doi.org/10.1070/QE1996v026n09ABEH000788

[6] M. S. Isaev, U. T. Asatov, M. A. Tulametov, S. R. Kodirov, and A. E. Rajabov, "Study of the Inhomogeneities of Overcompensated Silicon Samples Doped with Manganese," East European Journal of Physics, (2), 341–344 (2024). https://doi.org/10.26565/2312-4334-2024-2-40

[7] J. S. Abdullayev, J. S. Abdullayev, I. B. Sapaev, J. I. Razzokov, D. A. Juraev, E. E. Elsayed, "Modeling of Optoelectronic Properties in p-Si/n-$Cd_mZn_{1-m}S$ Heterojunctions: Effects of Composition and Temperature," Journal of Electronic Materials, **54**, 11607–11617 (2025). https://doi.org/10.1007/s11664-025-12480-8

[8] A. T. Mamadalimov, M. S. Isaev, M. N. Mamatkulov, S. R. Kodirov, and J. T. Abdurazzokov, "Study of Silicide Formation in Large-Diameter Monocrystalline Silicon," East European Journal of Physics, (2), 366–371 (2024). https://doi.org/10.26565/2312-4334-2024-2-45

[9] M. S. Isaev, A. I. Khudayberdieva, M. N. Mamatkulov, U. T. Asatov, and S. R. Kodirov, "The Surface Layer Morphology of Si⟨Cr⟩ Samples," East European Journal of Physics, (4), 297–300 (2024). https://doi.org/10.26565/2312-4334-2024-4-32

[10] H. Wang, Z. Zhao, P. Liu, and X. Guo, "Laser-Induced Graphene Based Flexible Electronic Devices," Biosensors, **12**(2), 55 (2022). https://doi.org/10.3390/bios12020055

[11] C. Francis, A. Rektor, T. Valayil-Varghese, N. McKibben, I. Estrada, J. Forbey, and D. Estrada, "Laser-induced graphene gas sensors for environmental monitoring," Front. Chem. **12**, (2024). http://doi.org/10.3389/fchem.2024.1448205

[12] T. Han, A. Nag, R.B.V.B. Simorangkir, N. Afsarimanesh, H. Liu, S.C. Mukhopadhyay, and Y. Xu, *et al*., "Multifunctional Flexible Sensor Based on Laser-Induced Graphene," Sensors, **19**, 3477 (2019). https://doi.org/10.3390/s19163477

[13] X. Zhao, J. Zhai, Y. Zhou, J. Hu, and L. Wang, "Femtosecond laser-driven synthesis of laser-induced graphene: Optimizing microstructure and electrochemical performance for flexible electrodes," Journal of Colloid and Interface Science, **703**, Part 1 (2026). https://doi.org/10.1016/j.jcis.2025.139061

[14] M. R. Bedilov, I. Yu. Davletov, and Sh. D. Sultanov, "Charge and energy spectra of fast multicharged ions in a laser plasma," Plasma Physics Reports, **28**(12), 1038–1040 (2002). https://doi.org/10.1134/1.1528235

[15] R.T. Khaydarov, H.B. Beisinbaeva, M.M. Sabitov, Milan Kalal, and G.R. Berdiyorov, "Conditions defining the mechanisms of the formation of light gas ions in multicomponent laser-produced plasmas," Nuclear Fusion, **50**(10), 105007 (2010). https://doi.org/10.1088/0029-5515/50/10/105007

[16] M. Guan, Z. Zhang, W. Zhu, Y. Gao, S. Wang, and X. Li, "Femtosecond laser-induced graphene for temperature and ultrasensitive flexible strain sensing," Front. Mater. Sci. **18**(3), 240696 (2024). https://doi.org/10.1007/s11706-024-0696-6

[17] R. Murray, M. Burke, D. Iacopino, and A.J. Quinn, "Design of Experiments and Optimization of Laser-Induced Graphene," ACS Omega, **6**(26), 6736–16743 (2021). https://doi.org/10.1021/acsomega.1c00309

[18] G. S. Boltaev, M. Iqbal, S. R. Kamalov, M. Vapaev, I. Y. Davletov, and A. S. Alnaser, "Impact of plasma conditions on the shape of femtosecond laser-induced surface structures of Ti and Ni," Applied Physics A, **128**(6), 488 (2022). https://doi.org/10.1007/s00339-022-05614-w

[19] B. X. Eshchanov, G. I. Mukhamedov, N. S. Khalilova, B. R. Sobirov, M. Vapaev, G. S.Boltaev, "Ultrafast laser nanostructured silicon coated with silver nanoparticles for efficient SERS detection of R6G," Applied Physics A, **132**(2), 111 (2026). https://doi.org/10.1007/s00339-025-09179-2

[20] A. I. Japakov, M. E. Vapaev, R. M. Bedilov, Z. T. Azamatov, and I. Y. Davletov, "Spectra of Multiply Charged Ions in Laser Plasma Formed from Gas-Containing Targets," East European Journal of Physics, (3), 490-494 (2023). https://doi.org/10.26565/2312-4334-2023-3-55

[21] A. I. Japakov, R. M. Bedilov, J. O. Kamalova, I. Y. Davletov, and A. R. Matnazarov, "The impact of laser radiation frequency on the formation of the main characteristics of ions in a mono-element laser plasma," EPJ Web of Conferences, **318**, 05002 (2025). https://doi.org/10.1051/epjconf/202531805002

[22] M. E. Vapaev, F. M. Tojinazarov, B. R. Sobirov, S. R. Kamalov, I. Y. Davletov, and G. S. Boltaev, "Laser fluence-dependent LIPSS formed on the surface of niobium alloys," EPJ Web of Conferences, **318**, 05005 (2025). https://doi.org/10.1051/epjconf/202531805005

[23] M. Akhmedov, J. Sadullayev, M. Vapayev, A. Matnazarov, I. Davletov, and J. Rayimbaev, "Picosecond-pulsed laser ablation of aluminum foils: crater morphology and plasma parameters," Engineering Research Express, **7**(3), 035362 (2025). https://doi.org/10.1088/2631-8695/ae0092

[24] M. Akhmedov, J. Sadullayev, M. Vapayev, F. Tojinazarov, I. Davletov, and J. Rayimbaev, "Effects of picosecond pulsed laser radiation on crater formation on copper foil surfaces," Engineering Research Express, **8**, 035401 (2026). https://doi.org/10.1088/2631-8695/ae3b9d

[25] Z. Ruziev, U. Sapaev, H. Eshkuvatov, R. Karimov, I. Egamberdiev, M. Musurmonov, and R. Turniyazov, "Surface ionization of diamond by femtosecond laser pulses: A comparative study of analytical models," Results in Optics, **23**, 100942 (2026). https://doi.org/10.1016/j.rio.2025.100942

[26] F.F. Franco, M.H. Malik, L. Manjakkal, A. Roshanghias, C.J. Smith, C. Gauchotte-Lindsay, "Optimizing Carbon Structures in Laser-Induced Graphene Electrodes Using Design of Experiments for Enhanced Electrochemical Sensing Characteristics," ACS Appl. Mater. Interfaces, **16**(47), 65489–65502 (2024). https://doi.org/10.1021/acsami.4c13124

[27] COMSOL AB, "Modeling ultrafast heat transfer with COMSOL Multiphysics," COMSOL Blog, 2026. https://www.comsol.com/blogs/modeling-ultrafast-heat-transfer-with-comsolmph

[28] J. Fernandes, and M.-J. Kim, "Probing ultrafast heat transfer mechanisms in plasmonic gold nanostructures: FEM analysis of core–shell configurations under femtosecond laser irradiation," Phys. Chem. Chem. Phys. (23), (2025). https://doi.org/10.1039/D5CP00715A

[29] COMSOL AB, "Ultrafast heat transfer due to femtosecond laser heating," COMSOL Application Gallery, 2025. https://www.comsol.com/model/ultrafast-heat-transfer-due-to-femtosecond-laser-heating-142421

[30] J. S. Abdullayev, L. Abdullayeva, L. Agamalieva, and R. Ismailova, "Correlating Ni microstructure with Schottky barrier homogeneity in monolayer MoS_2 field-effect transistors," Advanced Physical Research, **7**(3), 350–357 (2025). https://doi.org/10.62476/apr.73350

[31] J. S. Abdullayev, and I. B. Sapaev, (2025). Analytic analysis of the features of GaAs/Si radial heterojunctions: Influence of temperature and concentration. East European Journal of Physics, (1), 204–210. https://doi.org/10.26565/2312-4334-2025-1-21

[32] J. S. Abdullayev, I. B. Sapaev, N. Esanmuradova, S. Kadirov, and Sh.M. Kuliyev, "Mathematical analysis of the features of radial p-n junction: Influence of temperature and concentration," East European Journal of Physics, (2), 220–225 (2025). https://doi.org/10.26565/2312-4334-2025-2-24

[33] A. Mustafoqulov, R. Baratov, Z. Radjapov, S. Kadirov, and B. Urinov, "Angular displacement measurement and control sensors of agricultural robot-manipulators," in: *IV International Conference on Agricultural Engineering and Green Infrastructure for Sustainable Development (AEGISD-IV 2024)*, **105**, 03003 (2024). https://doi.org/10.1051/bioconf/202410503003

[34] A. Y. Boboev, N. Y. Yunusaliyev, G. G. Tojiboyev, O. S. Muminov, and S. R. Kadirov, "SRIM simulation of irradiation damage by protons in ZnO: S compound," Journal of Ovonic Research, **21**(6), 781-788 (2025). https://doi.org/10.15251/JOR.2025.216.781

[35] A. Y. Boboev, U. Karimberdiev, S. Kadirov, and N. Y. Yunusaliyev, "Growth of Solid Solutions $(Ge_2)(GaAs_{1-\delta}Bi_{\delta})_x(ZnSe)_y$ on Silicon Substrates by Liquid Phase Epitaxy," Chalcogenide Letters, **22**(11), 951-957 (2025). https://doi.org/10.15251/CL.2025.2211.951

[36] A. T. Mamadalimov, M. S. Isaev, S. R. Kodirov, T. U. Atamirzaev, M. N. Mamatkulov, A. UT, "Comparative Analysis of the Properties of Manganese Silicide," J. Nano- Electron. Phys. **17**(5), 05011 (2025). https://doi.org/10.21272/jnep.17(5).05011

[37] S. R. U. Qodirov, and I. Y. Davletov, "Improving thinking and imagining skills in school students by training the physics using simulations," AIP Conference Proceedings, **3268**(1), 060006 (2025). https://doi.org/10.1063/5.0257234

[38] I. Davletov, N. Khakimov, A. Qodirov, M. Akhmedov, J. Sadullayev, and O. Khamraev, "Soft start of induction electric motors using rezistor and denistor devices," E3S Web of Conferences, **461**, 01066 (2023). https://doi.org/10.1051/e3sconf/202346101066

[39] I. Y. Davletov, N. Z. Khakimov, A. K. Qodirov, M. M. Akhmedov, J. O. Sadullayev, O. O. Khamraev, "Increasing the Efficiency of Asynchronous Motors by Improving the Quality of the Electric Current," in: *2023 IEEE XVI International Scientific and Technical Conference Actual Problems of Electronic Instrument Engineering (APEIE)*, (2023), pp. 1820-1824). https://doi.org/10.1109/APEIE59731.2023.10347842

[40] R.D. Crapnell, E. Bernalte, R. A. A. Muñoz, and C. E. Banks, "Electroanalytical overview: the use of laser-induced graphene sensors," Anal. Methods, **17**, 635-651 (2025). https://doi.org/10.1039/d4ay01793e

[41] C.H. Kim, J.H. Kim, S.Y. Jeong, and B.S. Shine, "Atomistic and data-driven modeling of laser-induced graphene formation on sustainable polymer substrates," Sci. Rep. **15**, 31627 (2025). https://doi.org/10.1038/s41598-025-15945-2

[42] S.V. Pavlov, "Defect Engineering in Laser-Induced Graphene (LIG) Through Temperature Control: A Reactive Molecular Dynamics Study," Molecules, **30**, 4344 (2025). https://doi.org/10.3390/molecules30224344

[43] J.O. Sadullayev, M.M. Akhmedov1, M.E. Vapayev, I.Y. Davletov, and G.S. Boltaev, "Modeling of Thermal Effects in a Polyimide Target Under Pulsed Laser Irradiation," East European Journal of Physics, (1), 274–280 (2026). https://doi.org/10.26565/2312-4334-2026-1-31

КІНЦЕВО-ЕЛЕМЕНТНЕ МОДЕЛЮВАННЯ ВПЛИВУ ШВИДКОСТІ СКАНУВАННЯ НА ФОРМУВАННЯ ГРАФЕНУ, ІНДУКОВАНОГО ФЕМТОСЕКУНДНИМ ЛАЗЕРОМ

Дж.О. Садуллаєв[1], **М.М. Ахмедов**[1], **М.Є. Вапаєв**[1], **А.Е. Раджабов**[1], **І.Й. Давлетов**[1], **Г.С. Болтаєв**[2]

[1]*Кафедра електротехніки та енергетики, Ургенчський державний університет імені Абу Райхана Беруні, Ургенч, 220100, Узбекистан*

[2]*Кафедра фізики, Американський університет Шарджі, Шарджа 26666, Об'єднані Арабські Емірати*

Індукований лазером графен (LIG) забезпечує безмаскове пряме записування провідних вуглецевих структур на підкладках із поліміду для застосувань у гнучкій електроніці та сенсорних системах. У випадку графену, індукованого фемтосекундним лазером (FLOG), швидкість сканування суттєво впливає на локальне температурне поле, а отже — на ступінь і якість графітизації, однак ця залежність досі не є повністю кількісно визначеною. У цьому дослідженні в середовищі COMSOL Multiphysics реалізовано нестаціонарну скінченно-елементну модель для визначення розподілу температури, що формується фемтосекундним лазерним пучком на поверхні поліміду залежно від швидкості сканування. Лазер описано як рухоме гаусівське поверхневе джерело тепла, а нестаціонарне рівняння теплопровідності розв'язується для відтворення надшвидкого нагрівання та охолодження під час серії імпульсів. Результати моделювання для швидкостей сканування в діапазоні 0,05–0,20 м/с показують, що зменшення швидкості призводить до зростання пікової температури та розширення зони термічного впливу, тоді як збільшення швидкості зменшує обидва ці параметри. Порівняння розрахованих пікових температур із порогами графітизації, наведеними в літературі для графену, отриманого з поліміду, дозволило визначити проміжне вікно швидкостей сканування, за якого тепловий бюджет є достатнім для формування графену без надмірного перегрівання та пошкодження матеріалу.Запропонована модельна схема є практичним інструментом для попереднього вибору параметрів фемтосекундного лазера та прискорення оптимізації процесів FLIG у виробництві гнучких графенових пристроїв.

Ключові слова: *графен, індукований лазером; поліімід; швидкість сканування; надшвидкий теплоперенос; рухоме гаусівське джерело тепла; кінцево-елементне моделювання; розподіл температури; вікно графітизації*